All-electron GW+Bethe-Salpeter calculations on small molecules

Daichi Hirose,* Yoshifumi Noguchi, and Osamu Sugino
Institute for Solid State Physics, The University of Tokyo, 5-1-5 Kashiwanoha, Kashiwa, Chiba 277-8581, Japan
(Received 26 December 2014; revised manuscript received 2 March 2015; published 13 May 2015)

Accuracy of the first-principles GW+Bethe-Salpeter equation (BSE) method is examined for low-energy excited states of small molecules. The standard formalism, which is based on the one-shot GW approximation and the Tamm-Dancoff approximation (TDA), is found to underestimate the optical gap of N_2, CO, H_2O, C_2H_4, and CH_2O by about 1 eV. Possible origins are investigated separately for the effect of TDA and for the approximate schemes of the self-energy operator, which are known to cause overbinding of the electron-hole pair and overscreening of the interaction. By applying the known correction formula, we find the amount of the correction is too small to overcome the underestimated excitation energy. This result indicates a need for fundamental revision of the GW+BSE method rather than adjustment of the standard one. We expect that this study makes the problems in the current GW+BSE formalism clearer and provides useful information for further intrinsic development beyond the current framework.

DOI: 10.1103/PhysRevB.91.205111 PACS number(s): 31.15.xp, 71.15.Qe, 71.35.−y

I. INTRODUCTION

The first-principles Green's-function method developed on the basis of the many-body perturbation theory has provided us with a post-density-functional theory (post-DFT) [1–3] approach to the excitation of a real material. The development was independently pioneered by Hybertsen *et al.* [4] and Strinati *et al.* [5,6]. They showed, for several semiconductors and insulators, that the band gap comparable to the experimental one can be obtained by using the GW approximation (GWA) [7,8] to describe the self-energy operator simply as a product of the one-particle Green's function (G) and the dynamically screened Coulomb interaction (W) within the random-phase approximation (RPA). Thereafter GWA has been successfully applied to wide variety of materials. Later, the GW approximation was applied to the self-energy operator appearing in the equation of motion of the two-particle Green's function, known as the Bethe-Salpeter equation (BSE) [9–14]. Application of the GW+BSE method was pioneered by Onida *et al.* [10] who demonstrated, for an isolated sodium tetramer, that the optical spectra comparable to the experimental one are successfully obtained by incorporating the excitonic effect beyond the one-particle picture. The GW+BSE method has now been recognized as one of the most reliable first-principles methods for the calculation of optical spectra.

Recently, numerical procedures to solve GW+BSE have been improved, and owing to the recent development of massively parallel computers, size of the target system has been increasing year by year, with the largest systems reported so far being the fullurene-porphyrin complexes [15], the aqueous DNA [16], and the zincbacteriochlorin-bacteriochlorin complexes [17]. The first-principles GW+BSE code to be used in this work [18–24] has been adapted to recent supercomputers and is capable of handling more than 100 atoms.

When the GW+BSE method developed for extended systems was applied to small molecules, some problems of the method were recognized [25–27]. Several attempts have been made to correct the problems as follows. The first one is to overcome the error introduced by using the local-density approximation (LDA) as the starting point [28,29]. The DFT-LDA has an intrinsic tendency to localize the empty states too much within the molecular region thereby stabilizing falsely an anion state of some small molecules. To overcome this problem, Rohlfing *et al.* [30] proposed a procedure to reconstruct the Kohn-Sham (KS) orbitals using the diagonal and off-diagonal matrix elements of the GW self-energy operator and showed that the procedure works successfully for a SiH_4 molecule. This procedure will be called "Procedure I ."

The second one, "Procedure II," is to go beyond the Tamm-Dancoff approximation (TDA), which neglects the coupling part of the electron-hole (e-h) interaction kernel, or the propagation of the e-h pairs at negative energies (i.e., antipairs). TDA has been often employed in the GW+BSE calculations as well as the time-dependent DFT (TDDFT) [31,32] calculations as an acceptable simplification of the computation, but there are still controversies regarding the accuracy of TDA. Ma *et al.* [33] pointed out that TDA in GW+BSE calculations breaks down for the photoactive yellow protein (PYP) whose lowest optical gap involves a $\pi \rightarrow \pi^*$ transition. They argued that the coupling term has a non-negligible contribution hence requiring the full kernel to reproduce the experiment. Grüning *et al.* [34] pointed out that TDA breaks down when the density oscillation involves creation of the e-h pairs and antipairs causing mixing of the excitonic and plasmonic states. TDA then predicts a qualitatively wrong polarization effect on the optical and electron energy-loss spectra of carbon nanotubes. On the contrary, Rocca *et al.* [35,36] recently demonstrated that TDA hardly affects the low-energy excitations for Si clusters and that, even for the high-energy excitations, TDA only affects the oscillator strength due to violation of the Thomas-Reiche-Kuhn sum rule. There is also an argument on inaccuracy of TDA within TDDFT [37].

The third one, "Procedure III," is to modify the over-screening error appearing in one-shot GWA (G_0W_0). The dependency of the starting points for G_0W_0 calculations has been investigated [28,29,38–40]. Especially, Rostgaard *et al.* [38] and Blase *et al.* [39,40] reported that the use of too small HOMO-LUMO gap causes overestimation of the dynamically

*hirose@issp.u-tokyo.ac.jp

screened Coulomb interaction W and then underestimation of the HOMO-LUMO gap of G_0W_0. (Here HOMO and LUMO stand for, respectively, the highest occupied and the lowest unoccupied molecular orbital.) As a handy way to avoid this overscreening problem, Blase *et al.* [27,39,40] suggested to use the Hartree-Fock (HF) orbital energy for the self-energy operator instead of the KS eigenvalue of LDA. This technique, called G_0W_0@HF_{diag}, was found to improve the original G_0W_0, called G_0W_0@LDA, but has not been applied to GW+BSE, thus it is left unanswered if the optical spectra will improve or not.

These correction schemes have been tested independently, but their performance has not been systematically compared. It is nontrivial how the corrections combined will further improve, overcorrect, or undercorrect the GW+BSE calculation.

In this study, we focus on typical molecules, N_2, CO, H_2O, C_2H_4, and CH_2O, and systematically investigate the aforementioned issues related to the overbinding, the overscreening, and the contribution of the (e-h) antipairs using the three procedures. We use our all-electron mixed basis program [18–24] for the GW+BSE calculation and compare the present results with the available experimental data as well as previous GW+BSE and TDDFT calculations. The study shows that the standard GW+BSE method systematically underestimates the optical gap by about 1 eV although the ionization potential is well reproduced by G_0W_0, and shows that the three procedures do not correct the error sufficiently, prompting in-depth reexamination of approximations used in diving the Bethe-Salpeter equation.

II. METHODOLOGY

A. Standard GW+BSE method

The one-particle Green' s function G satisfies the following Dyson-type equation of motion:

$$[H_0 + \Sigma(E)]G(E) = EG(E), \tag{1}$$

where H_0 is the Hamiltonian in the Hartree approximation. The above equation may be rewritten for the quasiparticle (QP) wave functions $|\psi_\nu^{\rm QP}\rangle$ instead of G,

$$\left[H_0 + \Sigma\left(E_\nu^{\rm QP}\right)\right]\left|\psi_\nu^{\rm QP}\right\rangle = E_\nu^{\rm QP}\left|\psi_\nu^{\rm QP}\right\rangle. \tag{2}$$

In GWA, the self-energy operator Σ is evaluated by a product of the Green' s function G and the dynamically screened Coulomb potential W within RPA,

$$\Sigma^{GW} = iGW. \tag{3}$$

Practically, Σ^{GW} is separated into the Fock (exchange) term $\Sigma_{\rm x} \equiv iGv$, where v is the bare Coulomb potential and the screening (correlation) term $\Sigma_{\rm c} \equiv iG(W - v)$. In practice, Eq. (2) is rewritten using the LDA wave functions $|\psi_\nu^{\rm LDA}\rangle$ as the basis. Assuming that the QP wave functions may be approximated by LDA ones, the QP energy within GWA of a state ν is given by

$$E_\nu^{GW} = E_\nu^{\rm LDA} + \left\langle\psi_\nu^{\rm LDA}\middle|\Sigma^{GW}\left(E_\nu^{GW}\right) - \mu_{\rm xc}^{\rm LDA}\middle|\psi_\nu^{\rm LDA}\right\rangle, \tag{4}$$

where $E_\nu^{\rm LDA}$ and $\mu_{\rm xc}^{\rm LDA}$ are the LDA-KS orbital energy of a state ν and the LDA exchange-correlation potential, respectively. When E_ν^{GW} is expanded around $E_\nu^{\rm LDA}$, the above equation becomes

$$E_\nu^{GW} = E_\nu^{\rm LDA} + Z_\nu\left\langle\psi_\nu^{\rm LDA}\middle|\Sigma^{GW}\left(E_\nu^{\rm LDA}\right) - \mu_{\rm xc}^{\rm LDA}\middle|\psi_\nu^{\rm LDA}\right\rangle, \tag{5}$$

where Z_ν is the renormalization factor defined as

$$Z_\nu = \left[1 - \frac{\partial\Sigma^{GW}(E)}{\partial E}\right]^{-1}_{E=E_\nu^{\rm LDA}}. \tag{6}$$

In the standard GW+BSE calculation, the following eigenvalue equation is solved to incorporate the excitonic effect:

$$RA = \Omega A, \tag{7}$$

where the eigenvector A is the e-h amplitude, the eigenvalue Ω is the excitation energy, and R is defined as follows:

$$R = \left(E_c^{GW} - E_v^{GW}\right) + 2K^{R,{\rm x}} + K^{R,{\rm d}}, \tag{8}$$

where $E_c^{GW}(E_v^{GW})$ is the QP energy at the empty (filled) level, $K^{R,{\rm x}}$ is the exchange interaction of the e-h pair composed of the bare Coulomb interaction only, and $K^{R,{\rm d}}$ is the direct interaction of the e-h pair composed of the screened Coulomb interaction including the dynamical effect. Our GW+BSE formalism is based on Ref. [30]. In particular, differing from the more commonly used static approximation, the dynamical excitonic effect is incorporated by using the generalized plasmon pole (GPP) model [4,41] [Eq. (20) of Ref. [30]] when evaluating the dynamically screened Coulomb interaction W at both the GW and the BSE levels. Note that the static approximation introduces errors both in the GW and the BSE calculation, but those errors tend to cancel each other because the screened interaction appears with opposite sign in these calculations.

B. Procedure I : Off-diagonal correction

In Eq. (2), If the LDA and QP wave functions are not the same, the QP states can be obtained by expanding the LDA states, $|\psi_\nu^{\rm QP}\rangle = \sum_{\nu'} c_{\nu\nu'}|\psi_{\nu'}^{\rm LDA}\rangle$, which leads to a QP Hamiltonian

$$H_{\nu\nu'}^{GW} = E_\nu^{\rm LDA}\delta_{\nu\nu'} + \left\langle\psi_\nu^{\rm LDA}\middle|\Sigma^{GW} - \mu_{\rm xc}^{\rm LDA}\middle|\psi_{\nu'}^{\rm LDA}\right\rangle. \tag{9}$$

We diagonalize the above Hamiltonian to reconstruct a new set of wave functions $\{\psi'_\nu\}$, thereby the subscript ν does not indicate the index of the KS eigenstate anymore [30]. This procedure is one step toward the right direction and is hence expected to improve the standard GW+BSE calculation.

C. Procedure II: Beyond the Tamm-Dancoff approximation

For Procedure II, we use the full e-h interaction kernel in the Fock space of the e-h pairs and antipairs, or the full BSE matrix, which is given by a 2×2 block matrix,

$$\begin{pmatrix} R & C \\ -C^* & -R^* \end{pmatrix}\begin{pmatrix} A \\ B \end{pmatrix} = \Omega\begin{pmatrix} A \\ B \end{pmatrix}. \tag{10}$$

The diagonal (or resonant) term is given as Eq. (8), and the off-diagonal (or the coupling) term is given as

$$C = 2K^{C,{\rm x}} + K^{C,{\rm d}}, \tag{11}$$

where $K^{C,\mathrm{x}}$ is the exchange interaction of the e-h antipair composed of the bare Coulomb interaction only and $K^{C,\mathrm{d}}$ is the direct interaction of the e-h antipair composed of the screened Coulomb interaction including the dynamical effect. Their matrix elements are defined as follows:

$$K^{R,\mathrm{d}}_{vc,v'c'}(\Omega) = -\sum_l \int d\boldsymbol{r}d\boldsymbol{r}'\psi^*_c(\boldsymbol{r})\psi_{c'}(\boldsymbol{r})\psi_v(\boldsymbol{r}')\psi^*_{v'}(\boldsymbol{r}')W_l(\boldsymbol{r},\boldsymbol{r}') \times\frac{\omega_l}{2}\left[\frac{1}{\omega_l-\left[\Omega-\left(E^{GW}_{c'}-E^{GW}_v\right)\right]}+\frac{1}{\omega_l-\left[\Omega-\left(E^{GW}_c-E^{GW}_{v'}\right)\right]}\right] \tag{12}$$

$$K^{C,\mathrm{d}}_{vc,c'v'}(\Omega) = -\sum_l \int d\boldsymbol{r}d\boldsymbol{r}'\psi^*_c(\boldsymbol{r})\psi_{v'}(\boldsymbol{r})\psi_v(\boldsymbol{r}')\psi^*_{c'}(\boldsymbol{r}')W_l(\boldsymbol{r},\boldsymbol{r}') \times\frac{\omega_l}{2}\left[\frac{1}{\omega_l-\left[\Omega-\left(E^{GW}_{v'}-E^{GW}_v\right)\right]}+\frac{1}{\omega_l-\left[\Omega-\left(E^{GW}_c-E^{GW}_{c'}\right)\right]}\right] \tag{13}$$

$$K^{R,\mathrm{x}}_{vc,v'c'} = \int d\boldsymbol{r}d\boldsymbol{r}'\frac{\psi^*_c(\boldsymbol{r})\psi_{c'}(\boldsymbol{r}')\psi_v(\boldsymbol{r})\psi^*_{v'}(\boldsymbol{r}')}{|\boldsymbol{r}-\boldsymbol{r}'|}, \tag{14}$$

$$K^{C,\mathrm{x}}_{vc,c'v'} = \int d\boldsymbol{r}d\boldsymbol{r}'\frac{\psi^*_c(\boldsymbol{r})\psi_{v'}(\boldsymbol{r}')\psi_v(\boldsymbol{r})\psi^*_{c'}(\boldsymbol{r}')}{|\boldsymbol{r}-\boldsymbol{r}'|}, \tag{15}$$

where ω_l is the plasmon frequency and $W_l(\boldsymbol{r},\boldsymbol{r}')$ is the screened interaction at the plasmon mode l. The interaction kernels K are explicitly given different superscripts R and C though they can be distinguished by the subscripts only.

In TDA the coupling between the resonance ($v \to c$) and the antiresonant ($c \to v$) terms is omitted, thereby reducing the BSE matrix in Eq. (10) into the 1×1 block only, i.e., $RA = \Omega A$ [Eq. (7)]. The details are given in the paper by Hirata *et al.* [42], while we follow the notation adopted in Ref. [33].

D. Procedure III: G_0W_0@HF$_{\mathrm{diag}}$

For the Procedure III, we use the Hartree-Fock-like orbital energies E^{HF}_ν defined by

$$E^{\mathrm{HF}}_\nu = E^{\mathrm{LDA}}_\nu + \left\langle\psi^{\mathrm{LDA}}_\nu\middle|\Sigma_{\mathrm{x}}-\mu^{\mathrm{LDA}}_{\mathrm{xc}}\middle|\psi^{\mathrm{LDA}}_\nu\right\rangle \tag{16}$$

instead of the LDA-KS orbital energies for constructing the GW self-enegy operator [39]. Differing from Procedure I, this procedure corrects the wave functions, while the orbital energies are left unchanged.

TABLE I. Cutoff parameters. Σ_{x}: Fock exchange; v: bare Coulomb; $(W-v)$: screening term.

	PWs (Ry)	Σ_{x} and v (Ry)	$(W-v)$ (Ry)	No. of levels
N_2	23.78	44.22	9.63	10 000
CO	28.30	70.95	9.63	10 000
H_2O	23.78	38.52	4.91	12 000
C_2H_4	15.92	38.52	4.91	4000
CH_2O	28.30	33.21	12.58	12 000

E. Convergence test

Our calculations are executed on our all-electron mixed basis program [18–24], in which the LDA wave function is expanded as a linear combination of plane waves (PWs) and numerical atomic orbitals (AOs). The GW+BSE method requires, in principle, all the information on electronic states including localized states in the core region and free electron states above the vacuum level. Our all-electron program can take those states into account. In the present study of low-energy excitations, however, we did not include excitations of core electrons.

We use an fcc supercell of size 21.21 Å for all molecules. We use the Coulomb cutoff technique [43–45] to eliminate spurious interactions with the image cells. Other parameters are listed in Table I for each molecule: We use the cutoff energy for the plane-wave basis set (PWs) to obtain the HOMO and LUMO energy of the DFT-LDA within 0.01 eV error. We use different cutoff energies for the Fock operator Σ_{x}, the bare Coulomb v, and the screening term $W-v$. We use a sufficiently large number of empty states. The convergence properties of N_2 molecules are shown in Figs. 1–5. We use the atomic geometries of the ground state optimized with use of B3LYP/6-311G* and the reference values with use of EOM-CCSD [46–48]/aug-cc-pVQZ by the GAUSSIAN09 program package.

III. RESULTS AND DISCUSSION

A. GW calculation and HOMO-LUMO gap

Figure 6 shows the ionization potential (IP) obtained by LDA, G_0W_0@LDA, and G_0W_0@HF$_{\mathrm{diag}}$. Though IP is commonly obtained from the δ SCF or the Slater's transition state theory in LDA, here we use the HOMO level of LDA just to show how G_0W_0@LDA corrects the KS eigenvalues.

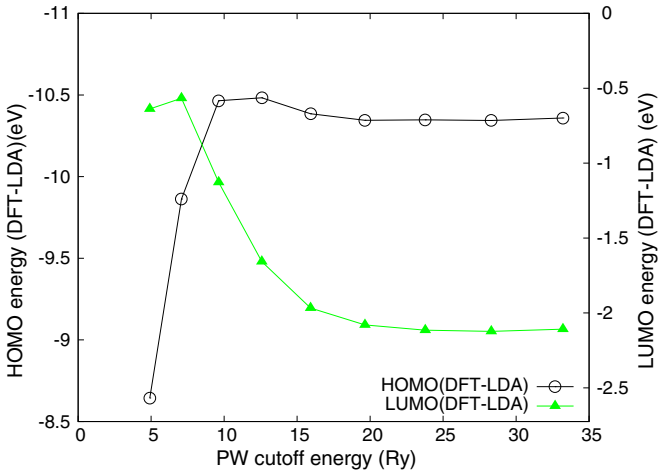

FIG. 1. (Color online) The HOMO and LUMO energies of DFT-LDA vs PW cutoff energy for a N_2 molecule.

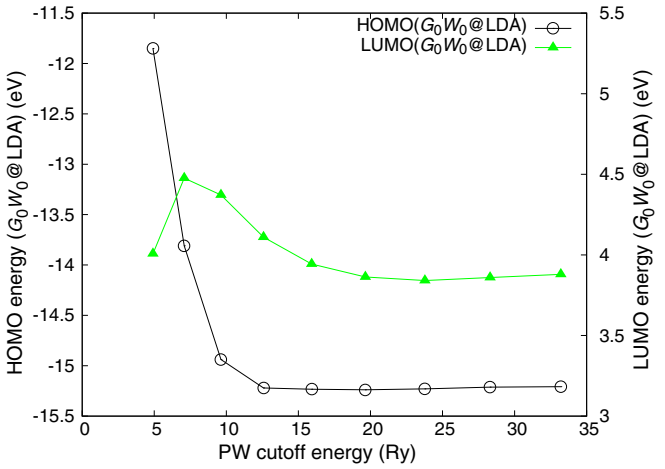

FIG. 2. (Color online) The HOMO and LUMO energies of G_0W_0@LDA vs PW cutoff energy for a N_2 molecule.

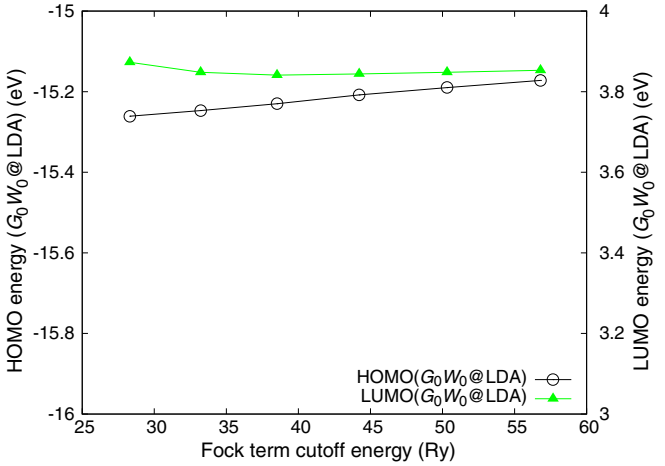

FIG. 3. (Color online) The HOMO and LUMO energies of G_0W_0@LDA vs cutoff energy for the Fock term. The calculation is done for a N_2 molecule.

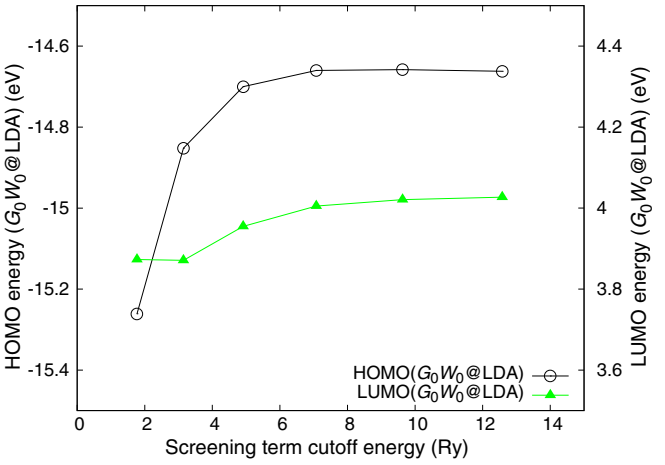

FIG. 4. (Color online) The HOMO and LUMO energies of G_0W_0@LDA vs cutoff energy for the screening term. The calculation is done for a N_2 molecule.

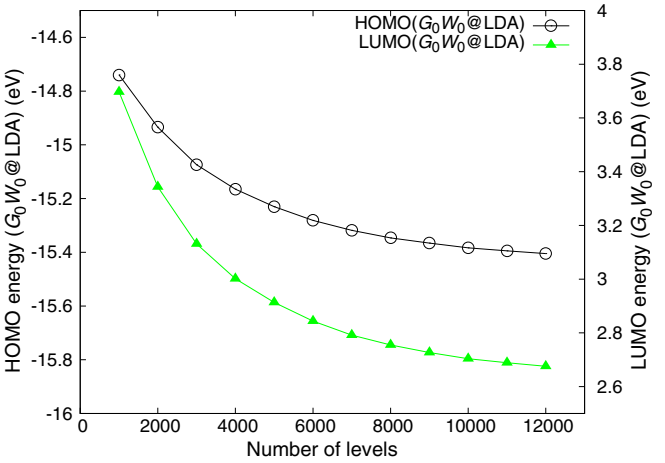

FIG. 5. (Color online) The HOMO and LUMO energies of G_0W_0@LDA vs number of levels for a N_2 molecule.

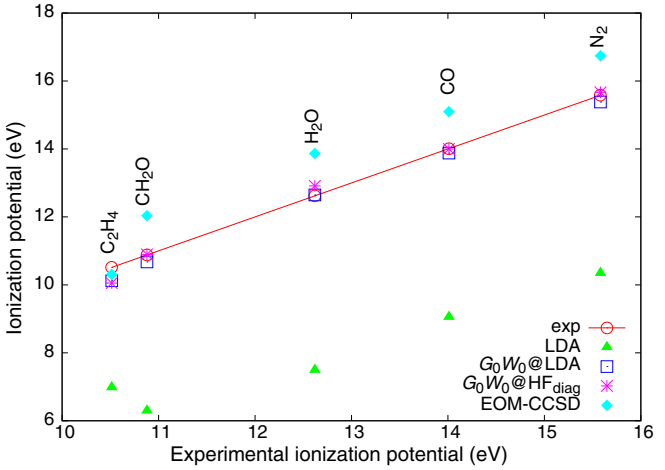

FIG. 6. (Color online) Comparison of the experimental and theoretical ionization potential. G_0W_0@LDA, G_0W_0@HF_{diag}, and EOM-CCSD calculations are shown with squares, asterisks, and rhombuses respectively, and HOMO levels of LDA (triangles) are shown for comparison.

TABLE II. Experimental and theoretical ionization potential in eV. MAE (in units of eV) is obtained from the absolute mean error.

	LDA	G_0W_0@LDA	G_0W_0@HF_{diag}	EOM-CCSD	Expt.
N_2	10.35	15.39	15.67	16.74	15.58 [49]
CO	9.06	13.88	14.00	15.10	14.01 [50]
H_2O	7.49	12.65	12.91	13.87	12.62 [51]
C_2H_4	6.99	10.12	10.05	10.31	10.51 [52]
CH_2O	6.30	10.68	10.90	12.04	10.88 [52]
MAE	4.68	0.19	0.17	0.74	

The IPs provided by the G_0W_0s are close to the experimental IPs as can be seen also from Table II, from which the mean absolute error (MAE) can be evaluated as 0.19 eV 0.17 eV, respectively, for G_0W_0@LDA and G_0W_0@HF_{diag}; MAE is 4.68 eV for the HOMO level of LDA. It is found that G_0W_0@HF_{diag} slightly improves over G_0W_0@LDA.

Note that the present LDA and G_0W_0@LDA IPs calculated for CO are consistent with the previously reported IPs in Ref. [53], though the IPs calculated for C_2H_4 are slightly different from those of Ref. [54] because an insufficient unit cell was used in Ref. [54].

Table III shows the HOMO-LUMO gaps evaluated by LDA, G_0W_0@LDA, G_0W_0@HF_{diag}. LDA provides a significantly underestimated HOMO-LUMO gap. Both G_0W_0s provide comparable values for the HOMO-LUMO gap, but G_0W_0@HF_{diag} provides generally larger values except for C_2H_4, where the values are different by less than 0.1 eV. From this G_0W_0 calculation, one might naturally expect that the G_0W_0@LDA+BSE and the G_0W_0@HF_{diag}BSE will provide almost comparable excitation energies while the latter will correct the former in the right direction; this will be verified below by performing the G_0W_0+BSE calculation. It might be also expected that, since the difference in IPs between G_0W_0@LDA and G_0W_0@HF_{diag} is at most 0.3 eV, the correction by Procedure III will not go beyond half an eV.

B. GW+BSE calculation and optical gap

Table IV shows the lowest two excitation energies obtained by the full BSE and TDA-BSE calculations starting both from G_0W_0@LDA and G_0W_0@HF_{diag}. First we emphasize that all the G_0W_0+BSE calculations underestimate the experimental excitation energy systematically by about 1 eV: This can be clearly seen from the value of MAE. Note that similar results

TABLE III. HOMO-LUMO gaps in eV for LDA, G_0W_0@LDA, G_0W_0@HF_{diag}, and EOM-CCSD.

	LDA	G_0W_0@LDA	G_0W_0@HF_{diag}	EOM-CCSD
N_2	8.23	18.09	18.36	18.68
CO	6.88	16.15	16.33	16.73
H_2O	6.58	13.40	13.73	14.60
C_2H_4	5.74	12.58	12.50	11.11
CH_2O	3.44	11.98	12.22	12.68

TABLE IV. The lowest two excitation energies in eV obtained from both G_0W_0@LDA and G_0W_0@HF_{diag}. The third column, TDA, refers to the results from the Tamm-Dancoff approximation while the fourth column, BSE, refers to those from the full BSE. Experimental results are from Ref. [42].

		G_0W_0@LDA		G_0W_0@HF_{diag}			
		TDA	BSE	TDA	BSE	EOM-CCSD	Expt.
N_2	S_1	7.93	7.93	7.76	7.69	9.47	9.31
	S_2	8.29	8.29	8.29	8.30	10.08	9.97
CO	S_1	7.69	7.67	7.59	7.62	8.62	8.51
	S_2	8.29	8.24	8.22	8.26	10.12	9.88
H_2O	S_1	6.43	6.43	6.65	6.65	7.66	7.4
	S_2	8.34	8.35	8.58	8.58	9.40	9.1
C_2H_4	S_1	6.01	6.01	5.97	5.97	7.50	7.11
	S_2	6.92	6.92	6.88	6.88	8.07	8.01
CH_2O	S_1	2.83	2.84	2.80	2.80	4.07	4.07
	S_2	6.37	6.37	6.62	6.62	7.30	7.11
MAE		1.14	1.14	1.11	1.11	0.18	

are reported. The standard G_0W_0+BSE method underestimates the optical gap of donor/acceptor molecular complexes, i.e., the associating tetracyanoetylene with benzene, toluen, o-xylene, napthalene by about 0.7 eV in gas phase [26] (0.4 eV near a metal surface [25]) and antracene derivatives by about 0.4 eV in gas phase [26]. However, they also showed that the error of optical gap reduces to 0.1–0.2 eV in the partial self-consistent GW+BSE calculation [26]. Although we performed this simple self-consistent procedure, the resulting excitation energies are hardly changed: the change in MAE is only within 0.01 eV.

In this context, we investigate below the reason why the excitation energies are underestimated by 1 eV although the ionization potentials are different from experiments by 0.1–0.2 eV using the aforementioned procedures. It should be mentioned here that such a large discrepancy is inherent only to small molecules where the excitonic effect is very important. Indeed, the exciton binding energies defined as the difference between the excitation energy and the QP gap are 5–12 eV, which is much larger than that of typical semiconductors, such as Si, where the binding energy is dozens of meV.

C. Effect of the Tamm-Dancoff approximation

We discuss the influence of TDA using Procedure II. Table IV shows that the difference between the full BSE and TDA is on the order of 10 meV, which is well within the numerical uncertainty of the present calculation. This is the case not only for the S_1 excitation but also for the S_2 excitation. The largest difference, 0.05 eV, can be seen in the S_1 excitation of CO, indicating that TDA is an excellent approximation. Note that the present results are consistent with the previous TDDFT calculations of small molecules [42].

Table V shows the exciton profile for the full BSE starting from G_0W_0@LDA. Since the HOMO-1 and LUMO of N_2 or CO are both doubly degenerated π orbitals, they are

TABLE V. Exciton profiles for the G_0W_0@LDA+BSE. The lowest two excitations S_1 and S_2 are projected into the noninteracting KS wave functions and the most important contribution, or the main transition, is shown with its projection amplitude of other terms constituting the BSE matrix. We refer to $K^{R,x}$ and $K^{C,x}$ as K^x together since they match up to 2 after the decimal point.

	Label	Main transitions $v \to c$	Ratio (%)	GW gap (eV)	$K^{R,d}$ (eV)	$K^{C,d}$ (eV)	K^x (eV)	R (eV)	C (eV)
N_2	S_1	HOMO-1(1)→LUMO(1)	48.6	19.06	–11.56	–0.39	0.40	8.31	0.42
		HOMO-1(2)→LUMO(2)	44.8	19.06	−11.56	–0.40	0.40	8.31	0.41
	S_2	HOMO→LUMO(1)	46.9	18.09	−11.56	–0.91	0.96	8.46	1.00
		HOMO→LUMO(2)	48.9	18.09	–11.55	–0.96	0.96	8.46	0.96
CO	S_1	HOMO→LUMO(1)	45.3	16.15	−11.18	–0.38	1.58	8.13	2.78
		HOMO→LUMO(2)	46.5	16.15	−11.18	–1.49	1.58	8.13	1.67
	S_2	HOMO-1(1)→LUMO(1)	49.8	18.89	−10.99	–0.09	0.37	8.65	0.65
		HOMO-1(2)→LUMO(2)	46.2	18.89	−10.99	–0.37	0.37	8.65	0.37
H_2O	S_1	HOMO→LUMO	77.4	13.40	−6.30	–0.18	0.18	7.46	0.18
		HOMO→LUMO + 1	16.1	13.17	−2.51	–0.04	0.04	10.75	0.04
	S_2	HOMO→LUMO + 2	64.4	13.86	−4.15	–0.04	0.04	9.78	0.04
		HOMO→LUMO + 15	24.8	15.52	−4.12	–1.70	0.06	11.52	−1.58
C_2H_4	S_1	HOMO→LUMO + 1	51.1	10.58	−9.05	–0.03	0.03	1.59	0.03
		HOMO→LUMO + 2	42.1	11.73	−2.96	–0.06	0.06	8.90	0.06
	S_2	HOMO-1→LUMO	14.3	14.75	−8.18	–0.29	0.30	5.18	0.32
		HOMO→LUMO + 4	60.9	11.82	−3.92	–0.03	0.03	7.96	0.03
		HOMO→LUMO + 16	16.4	13.25	−3.65	–0.04	0.04	9.68	0.04
CH_2O	S_1	HOMO→LUMO	98.5	11.98	−9.78	–0.37	0.37	2.93	0.37
	S_2	HOMO→LUMO + 1	48.4	11.18	−3.11	–0.05	0.05	8.16	0.05
		HOMO→LUMO + 2	26.4	12.31	−3.85	–0.14	0.13	8.71	0.12
		HOMO→LUMO + 3	16.7	12.23	−3.72	–0.05	0.05	8.60	0.05

indexed with (1) and (2). From Table V, we find that, in the resonant part, the direct interaction $K^{R,d}$ is an order of magnitude greater than the coupling $K^{C,d}$, except for the HOMO→LUMO + 15 transition of H_2O, where $K^{R,d}$ is 2.7 times larger. K^x is also small for N_2, H_2O, C_2H_4, and CH_2O. As a result, the ratio $|C/R|$ is small and thus TDA is justified. Note that K^x has relatively large values for the S_1 excitation of CO, yielding the largest value for the ratio $|C/R|$, which amounts to 34.2%, for the HOMO→LUMO(1) transition, but the effect on the excitation energy is quite small.

One may wonder how this conclusion is consistent with Ref. [34] which concluded a failure of TDA in describing the plasmon excitation of a carbon nanotube. This can be explained by the fact that the plasmon effect is negligible for molecules with a large HOMO-LUMO gap. Indeed, for the large Si clusters terminated with the hydrogen atoms, Rocca *et al.* [35,36] found that TDA hardly affects the low-energy excitation presumably because the plasmon excitation is restricted by the termination.

D. Comparison of G_0W_0@LDA and G_0W_0@HF_{diag}: Overscreening effect

Now, using Procedure III, we discuss the difference between G_0W_0@LDA and G_0W_0@HF_{diag}, or the effect of using a different starting point for the GW+BSE. Table IV shows that the optical gap of G_0W_0@HF_{diag}+BSE is slightly larger than that of G_0W_0@LDA+BSE and is closer to the experimental value. The improvement in MAE is, however, only 3%. And for S_1 excitation of N_2, the value is corrected in the opposite direction, indicating that G_0W_0@HF_{diag} does not always improve the optical gap.

Because of the overscreening effect, the GW gaps are generally underestimated and, at the same time, the attractive interaction between the electron and the hole (W) is also underestimated, while the bare Coulomb exchange interaction is unaffected. These underestimations cancel each other and weaken the QP energy dependence of the BSE gap. Indeed, from Table VI, it is seen that the difference in the excitation energy between G_0W_0@HF_{diag} and G_0W_0@LDA, or the Δ BSE gap, is generally small. The Δ BSE gap is either negative or positive depending on the excitations, which suggests a delicate nature of the cancellation. Note that the Δ BSE gap corresponds quite faithfully to the difference in the resonant term ΔR; this indicates small effect of TDA.

E. Effect of the off-diagonal correction

The excitation energy of G_0W_0@LDA obtained using Procedure I, or the off-diagonal correction, is shown in Table VII. For N_2 and CO, the correction clearly worsens the excitation energies while slight improvement can be found for H_2O and C_2H_4, indicating that Procedure III is not effective in improving the results. Note that the full BSE provides slightly better results than TDA, as reflected in the smaller MAE.

TABLE VI. Exciton profiles for the G_0W_0@HF_{diag}+BSE. All the data shown in the last four columns refer to the full BSE starting from G_0W_0@LDA, which are denoted with the "Δ" prefix. Δ BSE gap corresponds to the difference between G_0W_0@HF_{diag} and G_0W_0@LDA.

	Label	Main transitions $v \to c$	Ratio (%)	ΔGW gap (eV)	$\Delta K^{R,d}$ (eV)	ΔR (eV)	ΔBSE gap (eV)
N_2	S_1	HOMO-1(1)→LUMO(1)	50.6	0.02	−0.27	−0.24	−0.24
		HOMO-1(2)→LUMO(2)	48.4	0.02	−0.16	−0.14	
	S_2	HOMO→LUMO(1)	45.3	0.27	−0.25	0.02	0.01
		HOMO→LUMO(2)	48.9	0.27	−0.25	0.02	
CO	S_1	HOMO→LUMO(1)	45.4	0.18	−0.26	−0.08	−0.05
		HOMO→LUMO(2)	46.8	0.18	−0.26	−0.08	
	S_2	HOMO-1(1)→LUMO(1)	53.8	0.24	−0.23	−0.07	0.02
		HOMO-1(2)→LUMO(2)	44.0	0.24	−0.23	−0.07	
H_2O	S_1	HOMO→LUMO	76.8	0.33	−0.06	0.27	0.22
		HOMO→LUMO + 1	16.4	0.29	−0.02	0.27	
	S_2	HOMO→LUMO + 2	63.7	0.30	−0.02	0.28	0.23
		HOMO→LUMO + 15	25.1	0.31	−0.04	0.27	
C_2H_4	S_1	HOMO→LUMO + 1	51.2	−0.01	−0.01	−0.02	−0.04
		HOMO→LUMO + 2	41.9	0.20	−0.02	0.00	
	S_2	HOMO-1→LUMO	7.7	0.19	−0.14	0.05	−0.04
		HOMO→LUMO + 4	65.3	0.00	−0.03	−0.02	
		HOMO→LUMO + 16	17.8	0.01	0.00	−0.01	
CH_2O	S_1	HOMO→LUMO	98.5	0.24	−0.28	−0.04	−0.04
	S_2	HOMO→LUMO + 1	48.2	0.27	0.00	0.27	0.25
		HOMO→LUMO + 2	25.1	0.31	−0.01	0.30	
		HOMO→LUMO + 3	17.8	0.29	−0.02	0.27	

Rolhfing *et al.* demonstrated that the off-diagonal correction shifts the S_1 excitation energy upwards by 0.67 eV for SiH_4. However, it should be reminded that the standard G_0W_0+BSE method underestimates the excitation energy by 0.31 eV, yielding overestimation of the experiment 0.37 eV [30]. The result implies that the off-diagonal correction can become larger as the molecular size is increased but does not necessarily improve the calculation.

TABLE VII. The off-diagonal correction. The lowest two excitation energies in eV by applying the off-diagonal correction to G_0W_0@LDA+BSE.

		TDA	BSE	Expt.
N_2	S_1	6.56	6.71	9.31
	S_2	6.72	6.98	9.97
CO	S_1	5.50	5.98	8.51
	S_2	6.47	7.16	9.88
H_2O	S_1	6.96	7.32	7.4
	S_2	9.30	9.32	9.1
C_2H_4	S_1	6.53	6.53	7.11
	S_2	7.75	7.75	8.01
CH_2O	S_1	4.37	4.36	4.07
	S_2	5.86	5.86	7.11
MAE		1.55	1.35	

IV. SUMMARY AND CONCLUSION

We have seen that the excitation energies of small molecules are underestimated by the GW+BSE by 1 eV although the ionization potentials are accurately calculated by GWA with the error being 0.1–0.2 eV. We have investigated the reason by applying the existing correction schemes: (1) the correction of the diagonal element of the *e-h* interaction kernel using the HF orbital energy; (2) the full BSE scheme beyond the Tamm-Dancoff approximation; and (3) diagonalizing the GW self-energy operator to reconstruct the orbitals. In our case, the amount of the correction is not large enough to overcome the 1-eV error, and the results are such that one cannot expect accurate calculation even when they are applied altogether. To overcome this problem, it will be of primary importance to check in depth all the approximations used in deriving the Bethe-Salpeter equation.

ACKNOWLEDGMENTS

The present calculations are performed with supercomputers from the Institute for Solid State Physics, University of Tokyo. Y.N. was supported by Grant-in-Aid for Young Scientist (B) (Grant No. 23740288) and Grant-in-Aid for Scientific Research (C) (Grant No. 26400383) from Japan Society for The Promotion of Science (JSPS). This work was supported by the Strategic Programs for Innovative Research (SPIRE), MEXT, and the Computational Materials Science Initiative (CMSI), Japan.

[1] P. Hohenberg and W. Kohn, Phys. Rev. **136**, B864 (1964).
[2] W. Kohn and L. J. Sham, Phys. Rev. **140**, A1133 (1965).
[3] W. Kohn, Rev. Mod. Phys. **71**, 1253 (1999).
[4] M. S. Hybertsen and S. G. Louie, Phys. Rev. B **34**, 5390 (1986).
[5] G. Strinati, H. J. Mattausch, and W. Hanke, Phys. Rev. Lett. **45**, 290 (1980).
[6] G. Strinati, H. J. Mattausch, and W. Hanke, Phys. Rev. B **25**, 2867 (1982).
[7] L. Hedin, Phys. Rev. **139**, A796 (1965).
[8] L. Hedin and S. Lundqvist, in *Effects of Electron-Electron and Electron-Phonon Interactions on the One-Electron States of Solids*, edited by Frederick Seitz, David Turnbull, and Henry Ehrenreich, Solid State Physics Vol. 23 (Academic Press, 1970).
[9] G. Strinati, Phys. Rev. B **29**, 5718 (1984).
[10] G. Onida, L. Reining, R. W. Godby, R. Del Sole, and W. Andreoni, Phys. Rev. Lett. **75**, 818 (1995).
[11] G. Onida, L. Reining, and A. Rubio, Rev. Mod. Phys. **74**, 601 (2002).
[12] M. Rohlfing and S. G. Louie, Phys. Rev. Lett. **81**, 2312 (1998).
[13] M. L. Tiago and J. R. Chelikowsky, Solid State Commun. **136**, 333 (2005).
[14] G. Strinati, Riv. Nuovo Cimento Soc. Ital. Fis. **11**, 1 (1988).
[15] I. Duchemin and X. Blase, Phys. Rev. B **87**, 245412 (2013).
[16] H. Yin, Y. Ma, J. Mu, C. Liu, and M. Rohlfing, Phys. Rev. Lett. **112**, 228301 (2014).
[17] I. Duchemin, T. Deutsch, and X. Blase, Phys. Rev. Lett. **109**, 167801 (2012).
[18] S. Ishii, K. Ohno, Y. Kawazoe, and S. G. Louie, Phys. Rev. B **63**, 155104 (2001).
[19] S. Ishii, K. Ohno, Y. Kawazoe, and S. G. Louie, Phys. Rev. B **65**, 245109 (2002).
[20] Y. Noguchi, S. Ishii, K. Ohno, and T. Sasaki, J. Chem. Phys **129**, 104104 (2008).
[21] Y. Noguchi and K. Ohno, Phys. Rev. A **81**, 045201 (2010).
[22] Y. Noguchi, O. Sugino, M. Nagaoka, S. Ishii, and K. Ohno, J. Chem. Phys. **137**, 024306 (2012).
[23] Y. Noguchi, O. Sugino, H. Okada, and Y. Matsuo, J. Phys. Chem. C **117**, 15362 (2013).
[24] Y. Noguchi, M. Hiyama, H. Akiyama, and N. Koga, J. Chem. Phys. **141**, 044309 (2014).
[25] J. M. Garcia-Lastra and K. S. Thygesen, Phys. Rev. Lett. **106**, 187402 (2011).
[26] X. Blase and C. Attaccalite, Appl. Phys. Lett **99**, 171909 (2011).
[27] P. H. Hahn, W. G. Schmidt, and F. Bechstedt, Phys. Rev. B **72**, 245425 (2005).
[28] F. Bruneval and M. A. Marques, J. Chem. Theory. Comput. **9**, 324 (2013).
[29] F. Caruso, P. Rinke, X. Ren, M. Scheffler, and A. Rubio, Phys. Rev. B **86**, 081102 (2012).
[30] M. Rohlfing and S. G. Louie, Phys. Rev. B **62**, 4927 (2000).
[31] E. Runge and E. K. U. Gross, Phys. Rev. Lett. **52**, 997 (1984).
[32] E. K. U. Gross and W. Kohn, Phys. Rev. Lett. **55**, 2850 (1985).
[33] Y. Ma, M. Rohlfing, and C. Molteni, Phys. Rev. B **80**, 241405 (2009).
[34] M. Grüning, A. Marini, and X. Gonze, Nano. Lett. **9**, 2820 (2009).
[35] D. Rocca, D. Lu, and G. Galli, J. Chem. Phys. **133**, 164109 (2010).
[36] D. Rocca, M. Voros, A. Gali, and G. Galli, J. Chem. Theory. Comput. **10**, 3290 (2014).
[37] A. Chantzis, A. D. Laurent, C. Adamo, and D. Jacquemin, J. Chem. Theory Comput. **9**, 4517 (2013).
[38] C. Rostgaard, K. W. Jacobsen, and K. S. Thygesen, Phys. Rev. B **81**, 085103 (2010).
[39] X. Blase, C. Attaccalite, and V. Olevano, Phys. Rev. B **83**, 115103 (2011).
[40] C. Faber, C. Attaccalite, V. Olevano, E. Runge, and X. Blase, Phys. Rev. B **83**, 115123 (2011).
[41] W. G. Aulbur, L. Jönsson, and J. W. Wilkins, Solid State Phys. **54**, 1 (2000).
[42] S. Hirata and M. Head-Gordon, Chem. Phys. Lett. **314**, 291 (1999).
[43] C. A. Rozzi, D. Varsano, A. Marini, E. K. U. Gross, and A. Rubio, Phys. Rev. B **73**, 205119 (2006).
[44] J. Spencer and A. Alavi, Phys. Rev. B **77**, 193110 (2008).
[45] F. Hüser, T. Olsen, and K. S. Thygesen, Phys. Rev. B **87**, 235132 (2013).
[46] J. F. Stanton and R. J. Bartlett, J. Chem. Phys. **98**, 7029 (1993).
[47] M. Caricato, G. W. Trucks, M. J. Frisch, and K. B. Wiberg, J. Chem. Theory Comput. **7**, 456 (2011).
[48] R. J. Bartlett and M. Musiał, Rev. Mod. Phys. **79**, 291 (2007).
[49] T. Trickl, E. Cromwell, Y. Lee, and A. Kung, J. Chem. Phys. **91**, 6006 (1989).
[50] P. Erman, A. Karawajczyk, E. Rachlew-Källne, C. Strömholm, J. Larsson, A. Persson, and R. Zerne, Chem. Phys. Lett. **215**, 173 (1993).
[51] R. H. Page, R. J. Larkin, Y. Shen, and T. Lee, Yuan, J. Chem. Phys. **88**, 2249 (1988).
[52] K. Ohno, K. Okamura, H. Yamakado, S. Hoshino, T. Takami, and M. Yamauchi, J. Phys. Chem. **99**, 14247 (1995).
[53] Y. Noguchi, S. Ishii, and K. Ohno, J. Electron. Spectrosc. Relat. Phenom. **156-158**, 155 (2007).
[54] Y. Noguchi, S. Ishii, K. Ohno, I. Solovyev, and T. Sasaki, Phys. Rev. B **77**, 035132 (2008).